Safety and Reliability – Safe Societies in a Changing World – Haugen et al. (Eds)
© 2018 Taylor & Francis Group, London, ISBN 978-0-8153-8682-7

Integrated deterministic and probabilistic safety assessment of the cooling circuit of a superconducting magnet for nuclear fusion applications

R. Bellaera, R. Bonifetto, N. Pedroni, L. Savoldi & R. Zanino
NEMO group, Dipartimento Energia, Politecnico di Torino, Torino, Italy

F. Di Maio & E. Zio
Dipartimento di Energia, Politecnico di Milano, Italy

E. Zio
Chair on Systems Science and the Energetic Challenge, European Foundation for New Energy—Fondation EdF, CentraleSupelec, France

ABSTRACT: In recent years, there has been a growing interest in nuclear fusion as energy source due to its several principle advantages over fission, which include reduced radioactivity in operation and in waste, large fuel supplies, and increased safety. The most promising configuration of a nuclear fusion system is currently the tokamak, the largest of which, called the largest of which (ITER), is under construction in Cadarache, France. The safety of nuclear fusion systems has to be proved and verified by a systematic analysis of the system behavior under normal transient and accidental conditions. One challenge to the analysis is that the operation of tokamaks presents complex dynamic features as it is based on the transformer principle: in particular, they employ superconducting magnets, a subset of which operates with variable current to generate one of the components of the magnetic field needed to confine the plasma in the chamber where nuclear fusion reactions occur. In the present paper, we apply techniques of Integrated Deterministic and Probabilistic Safety Assessment (IDPSA), which combine phenomenological models of system dynamics with stochastic process models, taking for the first time as reference system the cooling circuit of a superconducting magnet for fusion applications, subject to a Loss-Of-Flow-Accident (LOFA).

1 INTRODUCTION

The need of satisfying a growing demand of energy, while protecting the environment and reducing the dependence on fossil fuels, has recently increased the interest in the use of nuclear fusion as energy source. Nuclear fusion presents several advantages over fission, which include reduced radioactivity in operation and in waste, large fuel supplies, and increased safety (EC, 2004).

The most promising configuration for electrical energy production from fusion is the tokamak, the largest of which (ITER) is now under construction at Cadarache (France), under an international collaboration between seven member entities (i.e., China, the European Union, India, Japan, Korea, Russia and the United States) (ITER, 2014).

Nuclear fusion reactors will use superconducting (SC) magnets to generate a powerful magnetic field needed to confine the plasma in the shape of a torus, where D-T fusion reactions occur at a temperature of the order of 10^8 K. On the other hand, all the SC coils need to be cooled at cryogenic temperatures in order to avoid the quench of the magnets (i.e., the loss of their superconducting state) during operation: for example, the ITER SC coils are cooled by supercritical helium (SHe) at a pressure of 0.5–0.6 MPa and temperature of about 4.5K (ITER, 2014). Dedicated cryogenic cooling loops remove the heat load from the magnets, releasing it to saturated liquid helium (LHe) pools, acting as thermal buffers in the transfer of the load to the refrigerator (Hoa et al., 2012; Zanino et al., 2013).

The safety of nuclear fusion systems has to be proved and verified by a systematic analysis of the system behavior under normal transient and accidental conditions (Taylor and Cortes, 2014; Rivas et al., 2015; Perrault, 2016; Wu et al., 2016), for two main reasons. First, the presence of radioactive sources (e.g., tritium and materials activated by the neutrons produced by the fusion reactions)

imposes a careful study to avoid the contamination of the workers, the public and the environment (Taylor, 2015; Taylor et al., 2017). Second, in view of the cost of the SC magnet system (Mitchell et al., 2008 and 2012), its protection and integrity should be guaranteed (ITER, 2014; Savoldi Richard et al., 2014; Savoldi et al., 2017 and 2018).

One challenge to the related safety analyses is that the operation of tokamaks presents *complex dynamic features*, as it is based on the transformer principle. In particular, they employ SC magnets, a subset of which operates with *variable* current to generate one of the components of the magnetic field needed to confine the plasma in the chamber where nuclear fusion reactions occur (Zohm, 2014). The *order* and *timing* of failure events occurring along an accident scenario, the *magnitude* of failures and the *values* of the process variables at the time of event occurrence are critical in determining the evolution of the system response (Aldemir, 2013; Kirschenbaum et al., 2009; Zio and Di Maio, 2009, 2010; Zio et al., 2010; Zio, 2014; Turati et al., 2017 and 2018).

To perform the safety assessments we resort to the Integrated Deterministic and Probabilistic Safety Assessment (IDPSA) framework (Di Maio et al., 2016) to combine (deterministic) phenomenological models of system dynamics with (probabilistic) stochastic process models. The IDPSA methodology is here used for the first time to analyze the response—to abnormal transient conditions—of the cooling system of a SC magnet, namely a *single* ITER Central Solenoid Module (CSM) in a reference (cold) *test facility* (Spitzer et al., 2015). In particular, a Loss-Of-Flow Accident (LOFA) is considered as reference abnormal scenario. The 4C code (Savoldi Richard et al., 2010) is employed for the (deterministic) simulation of the system behavior. Multiple Value Logic (MVL) is adopted for the description of the components failures (Garibba et al., 1985). The MVL allows describing that the components can fail at any time along the scenario, with *different* (discrete) *magnitudes* (Di Maio et al., 2015; Zio, 2013).

The paper is organized as follows. In Section 2, the single ITER CSM in the cold test facility is presented together with the corresponding simulator. In Section 3, the different regimes of system operation are described. The components failures causing the deviations from the nominal CSM conditions in the test facility are described in detail in Section 4, together with the use of MVL for generating accident scenarios. In Section 5, the results obtained are illustrated and analyzed. Finally, conclusions are drawn and summarized in Section 6.

2 DESCRIPTION OF THE SYSTEM AND PRESENTATION OF THE SIMULATOR

The ITER CS allows inducing the current in the plasma and maintaining it during long plasma pulses. It is composed by 6 CS modules (CSM) stacked in the vertical direction; each of them is being manufactured and will be independently tested. Each module is composed by 7 pancake-wound conductors, namely 6 hexa-pancakes and 1 quad-pancake. Each pancake is cooled in parallel, resulting in 40 parallel cooling channels per module, each featuring 14 turns. The He inlets are located at the coil bore, while the outlets are at the outer side of the magnet. All the pancakes of each module are electrically connected in series through suitable joints (Libeyre et al. 2015).

The main components of a reference facility for the CSMs *cold tests* (which is the subject of the present analysis) are the He refrigerator, producing the supercritical He (SHe) at 4.5 K, which is used to cool the magnets during the tests, and the test chamber where the module will be put into a cryostat. Besides these two main components, several manifolds, pipelines, heat exchangers (HXs) control valves (CV) of the cryoplant and a liquid He (LHe) thermal buffer will connect the refrigerator to the coil, and a dedicated power supply system will provide a current up to ~50 kA.

From the hydraulic point of view, the analysis reported here is focused on the loop cooling a single CSM. This closed loop, much simpler than that foreseen in ITER for the cooling of the CS, provides SHe at ~4.5 K to the inlets of the 40 hydraulic paths, collects the (warmer) SHe at their outlets and by means of a cold circulator drives it to two HXs, where the heat removed from the coil is transferred to a LHe buffer. The LHe evaporated in the buffer is, then, extracted and cooled down by the refrigerator.

The 4C thermal hydraulic code (Savoldi Richard et al. 2010) is used here to model both the coil and its SHe cooling loop. Figure 1 shows a scheme of the loop model. The SHe at the outlet of the cold circulator is cooled in HX1 to remove the heat generated by the compression process. Then, it is driven to the coil inlets through CV1 (fully open in normal operation) and a supply cryoline (cryoline 1). At the coil outlet, the SHe reaches HX2 through a return cryoline (cryoline 2) and CV2 (fully open in normal operation). The main input parameters of each component model are reported in Table 1. For the details of the model of each component, please refer to (Bonifetto et al. 2012) and (Zanino et al. 2013). A realistic characteristic of the cold circulator has been implemented in the circuit model, as described in detail in (Zanino et al. 2013) for another system.

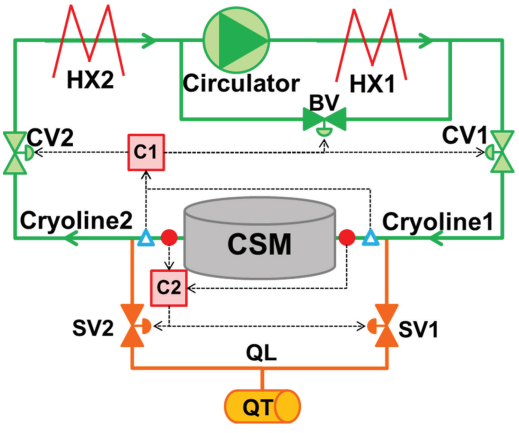

Figure 1. Scheme of the SHe cooling loop of the CSM. Solid red circles are pressure taps, open cyan triangles are flow meters (see the text for other abbreviations).

Table 1. Main input parameters of the circuit component models (L = length, D = diameter, K_v = flow coeffient).

Component	L [m]	D [mm]	# of parallel pipes
HX1,2	31	20	11
Cryoline1	28	46	
Cryoline2	24	46	
		K_v [m^3/h]	
CV1,2, BV, SVin, SVout		71	

With reference to a Loss-Of-Flow Accident (LOFA) (scenario of interest in the present paper, see the Introduction), the strategy adopted by the control system is assumed here to be similar to that adopted in ITER and described in (Savoldi et al., 2018) for the Toroidal Field (TF) coils. In particular, in order to protect the CS, a *controlled discharge* of the CS circuits is carried out in ITER, consisting of a *current ramp down* of about 30s (ITER_D_K7G8GN v2.1, 2014), driven by the plasma control system. Obviously, the current variation causes AC losses, which induce a (possibly significant) *heat deposition* in the conductor. In the reference system at hand, a similar fast controller discharge is assumed to be taken by the control system in case of LOFA. As far as the cryoplant is concerned, the basic circuit control in case of a LOFA includes the isolation of the circulator from the coil by means of the full closure of both CVs and the opening of the by-pass valve (BV) to equalize the pressure at the circulator suction and discharge (preventing any damage to the pump itself as fail-safe condition). In the present work, this action is taken (by controller C1 in Figure 1), when a SHe mass flow rate below 10% of the nominal value is measured both at the inlet and at the outlet of the CSM, after a validation time of 1s (Savoldi et al., 2018). Notice that the "nominal value" of the mass flow rate here considered corresponds to the nominal CSM conditions *during a test* in the reference facility, *not* to the "future" normal operating conditions in ITER. In case of excessive pressurization at the coil boundaries, two Safety Valves (SV) at the CSM inlet and outlet open, driven by the PID controller C2 (gain = 1 e^{-7}Pa^{-1}, integration time = 0.2 s, derivation time = 1 s), with set-point 1.8 MPa (Savoldi Richard et al., 2012); the controller parameters and set point have been assumed here equal to those in (Savoldi et al., 2018). When the SV opens, the He is released in a Quench Tank (QT) by means of suitable Quench Lines (QL).

The detailed CSM model solves the 1D transient mass, momentum and energy conservation equations, computing the temperature, pressure and velocity distribution, in each of the two regions (cable bundle and central, low impedance channel) of each pancake, as described in detail in (Zanino et al. 1995). Then, the inter-turn and inter-pancake thermal coupling between adjacent turns and pancakes, respectively, is computed considering the insulation as a thermal resistance to evaluate the heat transfer between neighboring conductors (Savoldi et al. 2000).

3 SYSTEM OPERATION REGIMES

During the tests, the facility and the CSM will be operated in different regimes, which can be briefly described as:

a. Cold mode standby operation (e.g. during night or weekend), when the CSM is not charged and kept at nominal ~4.5 K; no dangerous transients are expected from a LOFA in these conditions, so this regime is not analyzed here.
b. Cold mode experimental operation (i.e. during tests), when the CSM is charged at full or partial current (which is the case analyzed in the present paper). In this regime, an accidental temperature increase up to (or above) the so-called *current sharing temperature* T_{CS} may lead to a *quench*, i.e., to a loss of the superconducting state (notice that T_{CS} is defined as the temperature, above which the current starts to flow also in the Cu matrix of the SC strands and in the pure Cu strands, developing a non-zero voltage and causing Joule heat generation in the cable). The consequent fast local Joule heat deposition can induce thermal stresses that may seriously

damage the conductor, causing a degradation of its performance or, in the worst case, the loss of integrity of the conductor. The presence of a *normal* (non-SC) zone and, to some extent, variations in the conductor temperature above T_{CS} can be detected by measuring the voltage at the extremities of the each pancake.

The coil inlet temperature is here taken as the nominal one. The objective of the analysis is to study the response of the system described above (in the operating mode b.) to abnormal conditions, e.g., to accident scenarios driven by stochastic components failures (see the following Section 4). In particular, our interest is mainly devoted to LOFAs (see the previous Section 2). Actually, in absence of helium coolant flow, the heat deposition induced by AC losses (caused by the controlled discharge of the CS circuits) may a priori lead to a dangerous increase in the conductor temperature (with possible quench of the magnet), even in a cold test configuration like the one analyzed here. Two variables are monitored during each transient as "critical indicators" of the state of the system: the cooling helium pressure at the inlet and outlet of the CS magnet and the voltage measured at the coil extremities. Actually, if the pressure in the conductor exceeds 25 MPa, the conductors can be damaged (ITER_D_2NBKXY v1.2, 2009); also, if the voltage on a single pancake goes above 0.1 V for more than 1s, it means that the conductor temperature has exceeded the current sharing temperature T_{CS}, i.e., that the superconducting state of the magnet is lost.

4 FAILURE SCENARIOS GENERATION BY MULTIPLE VALUED LOGIC

The following component failures can occur at random times in the time horizon [0,600] seconds:

1. the Centrifugal Pump (CP) reduces exponentially the rotational speed, directly affecting the mass flow rate that can be reduced to i) 75%; ii) 50%; iii) 25%; iv) 0% of the nominal mass flow rate, i.e. in the last case down to a total loss of pumping capacity.
2. the two Control Valves (CVs) can fail in three different modes: i) stuck (open) at the nominal position; ii) stuck closed at 50% of the nominal position; iii) stuck totally closed.
3. the By-pass Valve (BV) can fail in three different modes: i) stuck (closed) in nominal position; ii) stuck open at 50% of the flow area; iii) stuck totally open.
4. the two Safety Valves (SVs) can fail in three different modes: i) stuck (closed) in nominal position; ii) stuck open at 50% of the flow area; iii) stuck totally open.

It can be shown that the system reaches a steady state condition in ~100 seconds, irrespectively of the failure occurred. Therefore, we set a mission time $T_M = 700$ s.

A Multiple Value Logic (MVL) scheme has been adopted to generate the accidental scenarios, considering the stochastic (discrete) time interval (t) of occurrence of component failures, their (discrete) magnitude (m) and the order (ord) of events along the sequence. The random realizations of the discretized time and magnitudes values are included into a sequence vector that represents a generated scenario to be simulated, [m_{cp}, t_{cp}, ord_{cp}, m_{cv1}, t_{cv1}, ord_{cv1}, m_{cv2}, t_{cv2}, ord_{cv2}, m_{bv}, t_{bv}, ord_{bv}, m_{sv1}, t_{sv1}, ord_{sv1}, ms_{v2}, ts_{v2}, ord_{sv2}] (Di Maio et al., 2017). The following values are considered:

- time (t) discretization: we use the label $t = 1, 2, 3, 4, 5$ and 6, for failures occurring in the intervals [0, 100] s, [101, 200] s, [201, 300] s, [301, 400] s, [401, 500] s, [501, 600] s, respectively; $t = 0$ means that the component does *not* fail within the T_M of the scenario and the value "NaN" is used to identify the respective (non-)failure order (ord) in the sequence vector of the accidental scenario. Notice that, even if the failure order (ord) may seem redundant in the MVL representation, it is actually used to discriminate between scenarios where different components fail in the *same* time *interval t*. Also, it is worth highlighting that, once a time *interval t* is identified by MVL, the *actual* time of component failure (used in the deterministic simulation of the accident scenario) is randomly sampled within the interval.
- Magnitude (m) discretization:
  - the CP magnitude is indicated with the label $m_{cp} = 1, 2, 3$ or 4 for failure states corresponding to an exponential decrease of the rotational speed down to 75%, 50%, 25% and 0% of the nominal value, respectively; if $m_{cp} = 0$, the component does not fail;
  - for each CV, the magnitude is indicated by the label $m_{cv} = 1$, 2 or 3 if the component stays stuck (open) at the nominal position, stuck closed at 50% of the nominal position and stuck closed, respectively; if $m_{cv} = 0$, the component works correctly;
  - the BV magnitude is indicated by the label $m_{bv} = 1$, 2 or 3 if the component stays stuck in (closed) nominal position, stuck open at 50% of nominal flow area and stuck totally open, respectively; if $m_{bv} = 0$, the component does not fail;
  - for each SV, the magnitude is indicated by the label $m_{sv} = 1$, 2 or 3 if the component stays stuck (closed) in nominal position, stuck open at 50% of nominal flow area and stuck totally open, respectively; if $m_{sv} = 0$, the component works in that scenario.

As an example, the accidental sequence vector [4, 6, 5, 0, 0, NaN, 1, 2, 1, 2, 4, 3, 2, 5, 4, 1, 3, 2] represents a scenario where: the CP fails completely to 0% of the nominal value at a time in [501,600] s (fifth event occurring along the sequence); the CV1 correctly works throughout T_M; the CV2 fails stuck (open) at the nominal position at a time in [101,200] s (first event occurring along the sequence); the BV fails stuck open at 50% of the nominal flow area (third event along the sequence) at a time in [301,400] s; the SV1 fails stuck open at 50% of the flow area at a time in [401,500] s (fourth event along the sequence); finally, the SV2 fails stuck (closed) in nominal position at a time in [201,300] s (second event along the sequence).

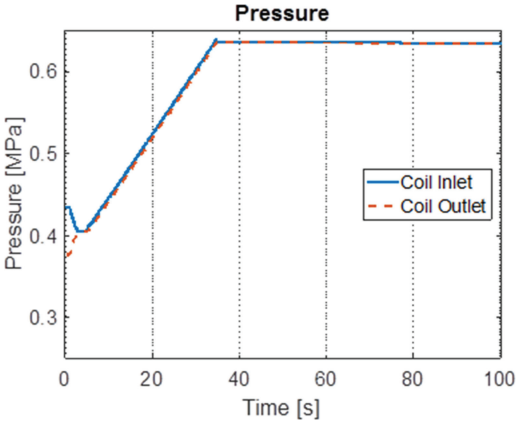

Figure 2. Pressure at the inlet and outlet of the coil (following the CP failure at 0% of the nominal mass flow rate).

5 RESULTS

In principle, the MVL accidental scenario generation procedure described above would entail the creation of 4×10^8 scenarios. We report here only the "bounding analysis" of the system response, analyzing a *reduced set* of MVL sequences, which are *expected* to be the *most challenging* for the system safety. Notice that *none* of the selected accident sequences turns out to be *critical* for the CS module integrity. In particular, the voltage at the extremities of the SC coil will remain far below the threshold of 0.1V (i.e., the temperature of the conductor does not exceed the T_{CS}): this means that the magnet maintains its superconductive properties.

Let us consider the MVL sequence [4, 1, 1, 0, 0, NaN, 0, 0, NaN, 0, 0, NaN, 0, 0, NaN, 0, 0, NaN], which entails the pump to fail according to an exponential decrease of the rotational speed till complete stop; the other components work correctly during the scenario. This sequence has been chosen because in this system no CP redundancies are designed and, therefore, a CP unavailability might lead the CSM to critical conditions. Notice that when the loss of flow is detected (Section 2), in order to protect the CS, a controlled discharge of its electrical circuits is carried out, consisting of a current ramp down to 0 in about 30s. A significant heat is, thus, generated in the conductors, due to the AC losses produced by the fast current variation. Figure 2 shows that when the LOFA occurs, the pressure of the coil both at the inlet (solid line on Figure 2) and outlet (dashed line) increases up to 50% with respect to the nominal value, without however exceeding the pressure safety threshold of 1.8 MPa.

Two additional MVL that might deserve attention are [0, 0, NaN, 0, 0, NaN, 0, 0, NaN, 0, 0, NaN, 3, 1, 1, 0, 0, NaN] and [0, 0, NaN, 0, 0, NaN, 0, 0, NaN, 0, 0, NaN, 0, 0, NaN, 3, 1, 1]. These sequences entail the failure of safety valves SV1 and SV2, located respectively at the inlet and outlet of the coil, that have the function of keeping the pressure of the system below the critical value of 1.8 MPa in accidental situations. In normal operation, the pressure at the inlet of SV1 is equal to 0.433 MPa and at the outlet is 0.42 MPa, corresponding to the assumed pressure of the quench tank. If component SV1 fails, helium starts flowing in the quench line leading to the reduction of the pressure at the inlet of the coil (solid line in Figure 3): both the inlet and the outlet pressure of the coil decrease, the mass flow rate remains at its nominal value and a new steady state situation is reached with large safety margin with respect to the pressure safety threshold 1.8 MPa.

Sequence [0, 0, NaN, 0, 0, NaN, 0, 0, NaN, 0, 0, NaN, 0, 0, NaN, 3, 1, 1], instead, entails SV2 failure. In Figure 4, it can be seen that the pressure at the inlet of the valve is equal to 0.376 MPa (solid line) whereas at the outlet (dashed line) it is equal to the assumed pressure of the quench tank (i.e., 0.42 MPa). When valve SV2 opens, the pressure at the outlet of the coil increases up to 0.42 MPa. Since the CP is working correctly, the nominal pressure drop between the inlet and the outlet of the component is maintained. As a consequence, the increase in the outlet coil pressure is followed by an increase in the inlet coil pressure. Also in this case, a new steady state condition is reached with a large safety margin with respect to the pressure safety threshold of 1.8 MPa.

The relevance of the dynamic features is witnessed by the outcome of sequence [0, 0, NaN, 0, 0, NaN, 0, 0, NaN, 0, 0, NaN, 3, 1, 1, 3, 1, 2], whose evolution is shown in Figure 5. The first failure is represented by the SV1 stuck open. This causes a slight decrease in the pressure at the inlet

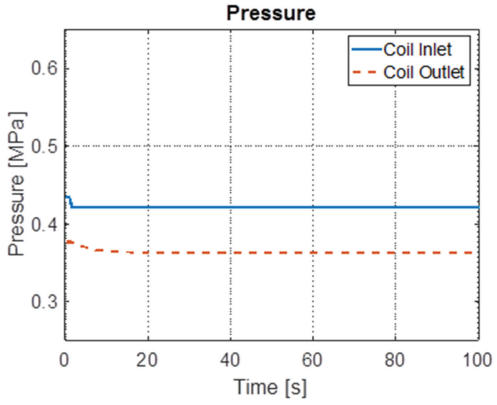

Figure 3. Pressure at the inlet and outlet of the coil following SV1 failure (stuck totally open).

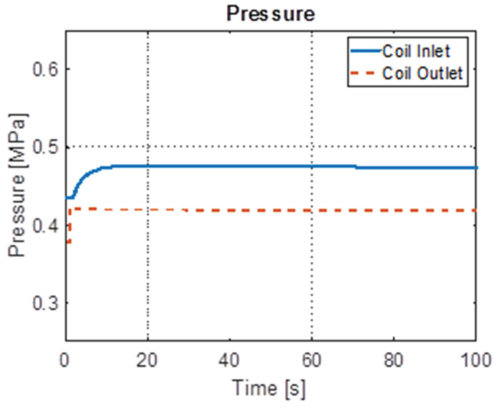

Figure 4. Pressure at the inlet and outlet of the coil following SV2 failure (stuck totally open).

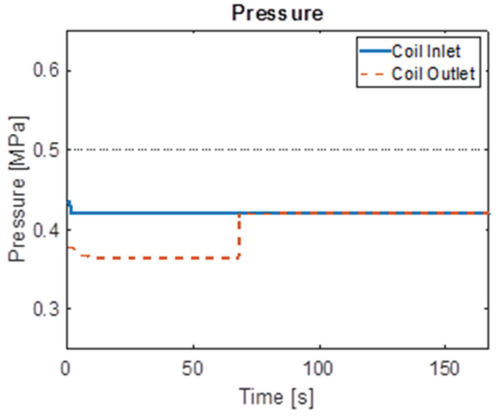

Figure 5. Pressure at the inlet and outlet of the coil along the sequence of failures: SV1 stuck totally open; SV2 stuck totally open.

(solid line) and at the outlet (dashed line) of the coil. Then, also safety valve SV2 fails stuck open, causing an increase in the pressure at the outlet of the coil up to the value of 0.42 MPa, the pressure assumed for the quench line (this is due to the fact that the pressure at the outlet of the coil is lower than that in the quench line). As a result, the pressure at the inlet and at the outlet of the coil equalizes: the LOFA happens (and is detected) and the current is reduced to zero producing AC losses, which lead to heat deposition. Throughout the rest of the transient, the value of the pressure at the boundaries of the coil stabilizes at 0.42 MPa. This response of the system justifies the necessity of a dynamic approach. In fact, if we consider the single failures of the SV1 and SV2 at the most conservative magnitude (see, e.g., Figures 3 and 4), a new steady state condition is reached *without* any *problem* from the point of view of the *availability* of the CSM in the test facility; on the other hand, the combination of failures considered just now leads to a different end state.

In all the scenarios reported here, the pressure at the boundaries of the SC coil is kept below the safety threshold of 1.8 MPa, i.e., with a positive safety margin. In other words, as for the analysis here presented, no critical situations are expected and the coil is not damaged. In addition, the voltage always stays well below the threshold of 0.1 V, which means that the current sharing temperature T_{CS} is not exceeded.

6 CONCLUSIONS

In this paper, we have considered the safety analysis of the simplified cooling system of a *single* module of the ITER Central Solenoid (CS) in a cold *test facility*, subject to a Loss-Of-Flow Accident (LOFA). For this, the deterministic 4C code has been employed to simulate the system behavior and a Multiple Value Logic (MVL) has been adopted for building a comprehensive set of combinations of times and (discrete) magnitudes of components failures to run stochastic accident scenarios. The cooling helium pressure at the inlet and outlet of the SC coil, and the voltage measured across the pancakes have been selected as "critical" safety parameters to monitor during each transient.

The application of the MVL has generated a list of more than 10^8 possible scenarios. However, for the sake of brevity, we have carried out only a "bounding analysis" of the system response by inspecting a *reduced set* of MVL sequences, in particular, those *expected* to be *most challenging* for the system safety. Results have shown that these scenarios are *not critical* for the CS module integrity: in particular, in all the cases considered, the

pressure at the boundaries of the SC coil is below the safety threshold of 1.8MPa, i.e., with a positive safety margin. Also, the voltage keeps well below the threshold of 0.1V, which means that the temperature of the conductor does not exceed the current sharing temperature T_{CS} and the magnet does *not* lose its SC properties.

However, a final remark is in order with respect to the positive results obtained. The CS magnet has been analyzed here in "cold mode experimental operation" (see Section 3), with the coil inlet temperature taken as the *nominal* one. In some cases, this temperature can be artificially increased, in order to perform specific tests (for example, the T_{CS} measurement (Savoldi et al. 2000)). This situation would reduce the temperature *margin* (namely, the difference between the operating cable temperature and the T_{CS}), shifting the operating point closer to the T_{CS} and, thus, reducing the amount of the heat needed to induce a quench. The analysis of such "more severe" operating conditions will be possibly considered in future research.

REFERENCES

Aldemir, T., 2013. A survey of dynamic methodologies for probabilistic safety assessment of nuclear power plants. *Ann. Nucl. Energy* 52: 113–124.

Bonifetto, R., Casella, F., Savoldi Richard, L., Zanino, R. 2012. *Dynamic modeling of a supercritical helium closed loop with the 4C code.* AIP Conference Proceedings (1434): 1743–1750.

Di Maio, F., Baronchelli, S., Zio, E., 2015. A computational framework for prime implicants identification in non-coherent dynamic systems. *Risk Analysis* 35(1): 142–156.

Di Maio, F., Vagnoli, M., Zio, E., 2016. Transient Identification by Clustering based on Integrated Deterministic and Probabilistic Safety Analysis Outcomes. *Annals of Nuclear Energy*, Volume 87, pp. 217–227, 2016.

Di Maio, F., Baronchelli, S., Vagnoli, M., Zio, E., 2017. Determination of Prime Implicants by Differential Evolution for the Dynamic Reliability Analysis of Non-Coherent Nuclear Components. *Annals of Nuclear Energy*, 102, pp. 91–105, 2017.

Garibba, S., Guagnini, E., Mussio, P., 1985. Multiple-Valued Logic Trees: Meaning and Prime Implicants. *IEEE Transactions On Reliability 34*: 463–472.

Hoa, C., Bon-Mardion, M., Bonnay, P., Charvin, P., Cheynel, J.N., Lagier, B., Michel, F., Monteiro, L., Poncet, J.M., Roussel, P., Rousset, B., Vallcorba-Carbonell, R., 2012. Investigations of pulsed heat loads on a forced flow supercritical helium loop—Part A: experimental set up. *Cryogenics*; 52(7–9): 340–8.

ITER, 2014. Central Interlock System Strategy for ITER Magnet Protection: Machine Protection Functions. Report *ITER_D_K7G8GN v2.1*, January 24, 2014.

ITER_D_2NBKXY v1.2, 2009. *ITER Design Description Document: Magnets—Conductors*, 09/09/2009.

ITER_D_K7G8GN v2.1, 2014. *Central Interlock System Strategy for ITER Magnet Protection: Machine Protection Functions*, January 24, 2014.

Kirschenbaum, J., Bucci, P., Stovsky, M., Mandelli, D., Aldemir, T., Yau, M., Guarro, S., Ekici, E., Arndt, S.A., 2009. A benchmark system for comparing reliability modeling approaches for digital instrumentation and control systems. *Nucl. Technol*. 165: 53–95.

Libeyre, P., Cormany, C., Dolgetta, N., Gaxiola, E., Jong, C., Lyraud, C., Reiersen, W., Everitt, D., Martovetsky, N., Rosenblad, P., Cole, M., Freudenberg, K., Sheng Liu, Smith, J., Jing Wei, Lin Wang, Xiaowu Yu, Xiaoyu Dong, Jijun Xin, Chao Li, Wangwang Zheng, Chao Fang 2015. Status of design and manufacturing of the ITER Central Solenoid and Correction Coils. *Proceedings of IEEE 26th Symposium on Fusion Engineering (SOFE)*: 1–8.

Mitchell, N., Bessette, D., Gallix, R., Jong, C., Knaster, J., Libeyre, P., Sborchia, C., Simon, F. 2008. The ITER magnet system. *IEEE Trans. Appl. Supercond*. 18: 435–440.

Mitchell, N., Devred, A., Libeyre, P., Lim, B., Savary, F. 2012. The ITER magnets: design and construction status. *IEEE Trans. Appl. Supercond*. 22: 4200809.

Perrault, D., 2016. Safety issues to be taken into account in designing future nuclear fusion facilities. *Fusion Engineering and Design* 109–111: 1733–1738.

Rivas, J.C., Dies, J., Fajarnés, X., 2015. Revisiting the analysis of passive plasma shutdown during an ex-vessel loss of coolant accident in ITER blanket. *Fusion Engineering and Design* 98–99: 2206–2209.

Savoldi, L., Bonifetto, R., Pedroni, N., Zanino, R. 2018. Analysis of a protected Loss Of Flow Accident (LOFA) in the ITER TF coil cooling circuit. *IEEE Transactions on Applied Superconductivity* 28(3): 4202009.

Savoldi Richard, L., Bonifetto, R., Bottero, U., Foussat, A., Mitchell, N., Seo, K., and Zanino, R., 2014. Analysis of the effects of the nuclear heat load on the ITER TF magnets temperature margin. *IEEE Trans. Appl. Supercond*. 24(3): Art. ID 4200104.

Savoldi Richard, L., Bessette, D., Bonifetto, R. and Zanino, R. 2012. Parametric analysis of the ITER TF fast discharge using the 4C code. *IEEE Trans. Appl. Supercond.* 22(3): Art. no. 4704104.

Savoldi Richard, L., Casella, F., Fiori, B., Zanino, R. 2010. The 4C Code for the Cryogenic Circuit Conductor and Coil modeling in ITER. *Cryogenics* (50): 167–176.

Savoldi, L., Bonifetto, R., Zanino, R., 2017. Analysis of a loss-of-flow accident (LOFA) in a tokamak superconducting Toroidal Field Coil. In: *Safety and Reliability—Theory and Applications, Proceedings of the ESREL 2017 Conference*; 18–22 June 2017; Portoroz, Slovenia; pp. 67–74; ISBN 9781138629370.

Savoldi, L., Zanino, R. 2000. Thermal-hydraulic analysis of TCS measurement in conductor 1A of the ITER central solenoid model coil using the M&M code. *Cryogenics* (40): 593–604.

Spitzer, J., Stephens, A., Schaubel, K., Smith, J., Norausky, N., Khumthong, K., Gattuso, A. 2015. ITER Central Solenoid Module fabrication program. *Proceedings of IEEE 26th Symposium on Fusion Engineering (SOFE)*: 1–6.

Taylor, N.P. 2015. Safety and licensing of nuclear facilities for fusion. *Proceedings of the 2015 IEEE 26th Symposium on Fusion Engineering (SOFE)*, 31 May-4 June 2015; Austin, TX, USA; DOI: 10.1109/SOFE.2015.7482293; ISBN: 978-1-4799-8264-6.

Taylor, N., Ciattaglia, S., Boyer, H., Coombs, D., Zhou Jin, X., Liger, K., Mora, J.C., Mazzini, G., Pinna, T., Urbonavicius, E., 2017. Resolving safety issues for a demonstration fusion power plant. *Fusion Engineering and Design* 124: 1177–1180.

Taylor, N., Cortes, P. 2014. Lessons learnt from ITER safety & licensing for DEMO and future nuclear fusion facilities. *Fusion Engineering and Design* 89: 1995–2000

Turati, P., Pedroni, N., Zio, E. 2017. Simulation-based exploration of high-dimensional system models for identifying unexpected events. *Reliability Engineering and System Safety* 165: 317–330.

Turati, P., Cammi, A., Lorenzi, S., Pedroni, N., Zio, E. 2018. Adaptive simulation for failure identification in the Advanced Lead Fast Reactor European Demonstrator. *Progress in Nuclear Energy* 103: 176–190.

Wu, Y., Chen, Z., Hu, L., Jin, M., Li, Y., Jiang, J., Yu, J., Alejaldre, C., Stevens, E., Kim, K., Maisonnier, D., Kalashnikov, A., Tobita, K., Jackson D., and Perrault, D., 2016. Identification of safety gaps for fusion demonstration reactors. *Nature Energy* 1: Article number: 16154.

Zanino, R., Bonifetto, R., Hoa, C., Savoldi Richard, L. 2013. 4C modeling of pulsed-load smoothing in the HELIOS facility using a controlled by-pass valve. *Cryogenics* (57): 31–44.

Zanino, R., De Palo, S., Bottura, L. 1995. A two-fluid code for the thermohydraulic transient analysis of CICC superconducting magnets. *Journal of Fusion Energy* (14): 25–40.

Zio, E. 2013. The Monte Carlo Simulation Method for System Reliability and Risk Analysis. London, UK: Springer.

Zio, E. 2014. Integrated deterministic and probabilistic safety assessment: Concepts, challenges, research directions. *Nuclear Engineering and Design* 280: 413–419.

Zio, E., Di Maio, F., 2009. Processing dynamic scenarios from a reliability analysis of a nuclear power plant digital instrumentation and control system. *Ann. Nucl. Energy* 36(9): 1386–1399.

Zio, E., Di Maio, F., 2010. A data-driven fuzzy approach for predicting the remaining useful life in dynamic failure scenarios of a nuclear power plant. *Reliab. Eng. Syst. Saf*. 95: 1: 49–57.

Zio, E., Di Maio, F., Stasi, M., 2010. A data-driven approach for predicting failure scenarios in nuclear systems. *Ann. Nucl. Energy* 37: 482–491.

Zohm, H., 2014. *Magnetohydrodynamic Stability of Tokamaks*. Wiley-VCH Verlag GmbH & Co. KGaA.